Molecular orbital calculation on the chemical bonding character of phosphate glasses

Y. Asano[1], S. Sakida[2], T. Nanba[1], Y. Miura[1]

[1]Department of Environmental Chemistry and Materials, Okayama University
3-1-1, Tsushima-Naka, Okayama 700-8530, Japan
[2]Health and Environment Center, Okayama University
3-1-1, Tsushima-Naka, Okayama 700-8530, Japan

Keywords : molecular orbital calculation, chemical bonding character, phosphate glass

Abstract

Chemical bonding character of various bonds in phosphate glasses was investigated on the basis of bond overlap population which was evaluated from molecular orbital calculations. Cluster models were constructed from various phosphate crystals. There are two terminal P–O bonds in phosphates, that is, P=O double bonds and P–NBO (non-bridging oxygen) bonds. In bond overlap population, P=O bonds were much larger than P–NBO bonds. In P=O bonds, no significant anti-bonding overlap between P and O was observed at around the HOMO levels, which was also the case in Si–NBO bonds. In resonance state between P=O and P–NBO bonds, which was seen in $(PO_{2/2}O_2)^-$ Q^2 unit, anti-bonding overlaps were clearly confirmed, which reduced the bond overlap population of terminal P–O bonds. In P–O–M bridges (M = B, Si, Ge and Al), more electrons were populated on P–O bonds than M–O bonds, which was due to the larger electronegativity of P atoms.

Introduction

Phosphate glasses have excellent physical properties such as low glass transition temperatures and high thermal expansion coefficients, and hence phosphate glasses have been applied to low-temperature sealing glasses. In pure P_2O_5 glass, glass networks consist of tetrahedral PO_4 units, where three oxygens are bridging oxygens (BOs) in P–O–P bridging bonds and the residual oxygen is doubly-bonded oxygen (DBO). The DBOs are located at the terminal of glass networks, which is similar to non-bridging oxygens (NBOs). In alkali or alkaline-earth oxides containing binary glasses, NBOs are also formed in the glasses. The NBOs are singly-bonded to phosphorous atoms, and hence they possess a negative unit charge. To compensate the negative charge of NBOs, alkali or alkaline-earth ions are bonded to NBOs to retain electroneutrality.

The authors' research group has studied electronic states and chemical bonding characters of various glasses mainly based on O1s X-ray photoelectron spectra (XPS) [1], where alkali phosphate glasses was also examined by XPS [2]. In the O1s XPS spectra, O1s signal was successfully separated into two components attributed to BO and DBO. After the alkali addition, however, a third new O1s component assigned to NBO was not observed. With increasing alkali content, the high binding energy component decreased and low binding energy component increased in relative intensity. The relative intensity of the low binding energy component was in good agreement with the total amount of DBO and NBO expected from the composition. It was consequently concluded that the DBO and NBO are in resonance state with each other [2]. Based on molecular orbital calculations, Uchino and Ogata reported that Li and Na ions

interacted equally with two terminal oxygens in a PO_4 unit but K and Rb ions interacted favorably with one of the two terminal oxygens [3], suggesting the resonance between DBO and NBO in lithium and sodium phosphate glasses and non-resonance in potassium and rubidium phosphate glasses. In either case, the terminal oxygens (TOs) are present in alkali or alkaline-earth phosphate glasses. TOs are very reactive as compared with BOs, and hence TO-abundant alkali phosphate glasses are easily soluble in water. Al_2O_3 are often added to improve chemical durability of phosphate glasses; tetrahedral AlO_4 units are formed and enter into the glass network, consuming TOs. Further addition of Al_2O_3 may be conducive to the formation of PO_4 units with no TOs, where PO_4 units with no TOs possess a unit positive charge, which is compensated by negatively-charged AlO_4 units. It is also the case in B_2O_3 addition to phosphate glasses. The situation is somewhat different in SiO_2 addition; due to the small addition of SiO_2, Si atoms enter into octahedral sites rather than tetrahedral sites.

Thus, in phosphate glasses, addition of various oxides leads to the structural changes not only of phosphate units but also of additives. At the same time, chemical bonding character of the glass constituents must be affected. In the present study, therefore, chemical bonding character of various phosphate systems was evaluated on the basis of molecular orbital calculations.

Computational method and cluster models

Molecular orbital calculations were performed by using the discrete variational Xα (DV-Xα) method [4], and chemical bonding characters were estimated by the Mulliken population analysis [5]. According to the Mulliken population analysis, chemical bonding character of a bond A–B was evaluated by the bond overlap population, Q_{AB},

$$Q_{AB} = 2 \sum_{i \in A, j \in B} Q_{ij}, \; Q_{ij} = \sum_{l} Q_{ij}^{l} \qquad (1)$$

$$Q_{ij}^{l} = n_l c_{il} c_{jl} S_{ij} \qquad (2)$$

where Q_{ij}^{l} is the partial overlap population, that is, electronic population of the overlapped region between the atomic orbitals χ_i and χ_j in the molecular orbital ϕ_l, which is the product of n_l: the number of electrons in MO ϕ_l (usually $n_l = 2$), c_{il} and c_{jl}: the contribution of atomic orbitals χ_i and χ_j in MO ϕ_l, and S_{ij}: the overlap integral between χ_i and χ_j.

Cluster models were constructed from the various phosphate crystals; pure P_2O_5 [6], alkali phosphates of Li_3PO_4 [7], $NaPO_3$ [8], $Na_5P_3O_{10}$ [9], KPO_3 [10], and $RbPO_3$ [11], aluminophosphates of $Al(PO_3)_3$ (Al = 6) [12], $NaAlP_2O_7$ (Al = 6) [13], and $AlPO_4$ (Al = 4) [14], and phosphates containing network forming oxides of BPO_4 (B = 4) [15], SiP_2O_7 (Si = 6) [16], and GeP_2O_7 (Ge = 6) [17], where the numbers in the parentheses indicate the coordination number. As shown in Figure 1, oxygen atoms in the respective crystals were placed at the center of the clusters, and MO_n polyhedra including the central oxygen were arranged around the central oxygen. The clusters were embedded in the Madelung potentials formed in the respective crystals to reduce the bond termination effect. The population analyses were done only for the bonds containing the central oxygens.

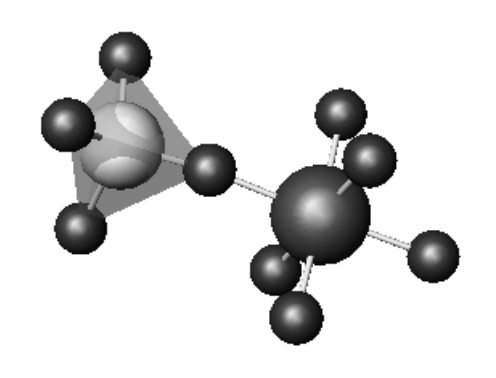

Figure 1: An example of cluster models.
P(4)–O–Al(6) constructed from $Al(PO_3)_3$ crystal.

Results and Discussion

Chemical Bonding Character of P_2O_5 and Alkali Phosphates

In P_2O_5 crystal [6], there are 2 phosphorous and 4 oxygen sites, in which the oxygen sites are classified into 2 BO and 2 DBO sites. Therefore, there are 4 distinct P–BO bonds and 2 distinct P=DBO bonds. As shown in Figure 2, the bond overlap population, Q_{PO} of P–BO bonds is widely distributed between 0.6 and 0.9, and it is also the case for P=DBO bonds. In a rough approximation, bond overlap population is inversely proportional to bond length. The wide distribution in Q_{PO} results from the wide distribution in P–O bond length; r(P–BO) = 0.1637, 0.1588, 0.1571, 0.1527 nm and r(P=DBO) = 0.1492, 0.1426 nm. As clearly seen in Fig. 2, Q_{PO} values of P=DBO bonds are larger than those of P–BO bonds, indicating that the P=O double bonds are stronger and more covalent than the P–O single bonds. The average Q_{PO} of P–BO bonds is 0.77, which is the largest among the conventional network formers of B_2O_3 ($Q_{B(3)O}$ = 0.64), SiO_2 ($Q_{Si(4)O}$ = 0.63) and GeO_2 ($Q_{Ge(4)O}$ = 0.54) [18] As for NBOs in sodium borate and silicate, $Q_{B(3)O}$ = 0.84 and $Q_{Si(4)O}$ = 0.85 [18]; Q_{PO} of P–TO bonds in sodium phosphates are much larger than those of terminal bonds in borate and silicate, which is due to the strong P=O double bond.

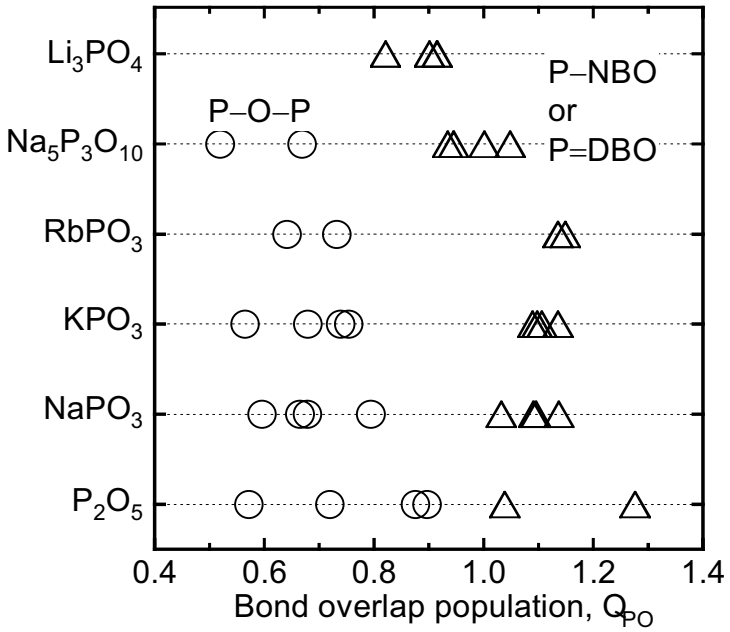

Figure 2: Bond overlap population, Q_{PO} of P–O bonds in

pure P_2O_5 and alkali phosphate crystals.

In $NaPO_3$ crystal [8], 4 of 6 oxygen sites are occupied by TOs, where the P–TO bond length narrowly ranges from 0.1484 to 0.1466 nm and TOs interact with 2 or 3 Na atoms at a distance between 0.2490 and 0.2350 nm. It is also the case in other alkali phosphate crystals. Thus, it is impossible to identify DBOs and NBOs in the alkali phosphate crystals examined in the present study. The bond orders of single and double bonds are 1 and 2, respectively. If P–NBO and P=DBO bonds were in non-resonant state, they would indicate different Q_{PO}. As shown in Fig. 2, however, Q_{PO} of P–TO bonds in $NaPO_3$ is narrowly distributed, suggesting the resonance between P–NBO and P=DBO bonds. As shown in Fig. 2, it is also the case in KPO_3 and $RbPO_3$; in these crystals, terminal oxygen atoms are crystallographically equivalent, and hence NBO and DBO are indistinguishable.

With increasing the relative amount of alkali oxides, P–BO and P–TO bonds both decrease in Q_{PO}, which is probably associated with the increase in the relative amount of TOs. In the case of sodium silicate [19], Q_{SiO} of Si–BO bonds decreased and that of Si–NBO bonds increased with increasing alkali content. Na ions in silicates interact with not only NBOs but also BOs, and the contribution of anti-bonding overlap between the atomic orbitals of Si and BO increased with increasing the number of Na ions associated to BO. In the case of Si–NBO bonds, however, the anti-bonding overlap was not confirmed at around HOMO levels, and Q_{SiO} of Si–NBO bonds increased with the increase of alkali content, which was opposite to the change of Q_{PO} of P–TO bonds. As shown in Figure 3(a), only small contribution of anti-bonding overlap was confirmed in the P=O bond. As shown in Figs. 3(a) ~ (c), however, the anti-bonding overlaps between the atomic orbitals of P and O are clearly recognized both in P–BO and P–TO bonds at around HOMO levels (0 ~ −5 eV). The anti-bonding overlap in P–TO bonds in alkali phosphates may be caused by the resonance between P–NBO and P=DBO bonds.

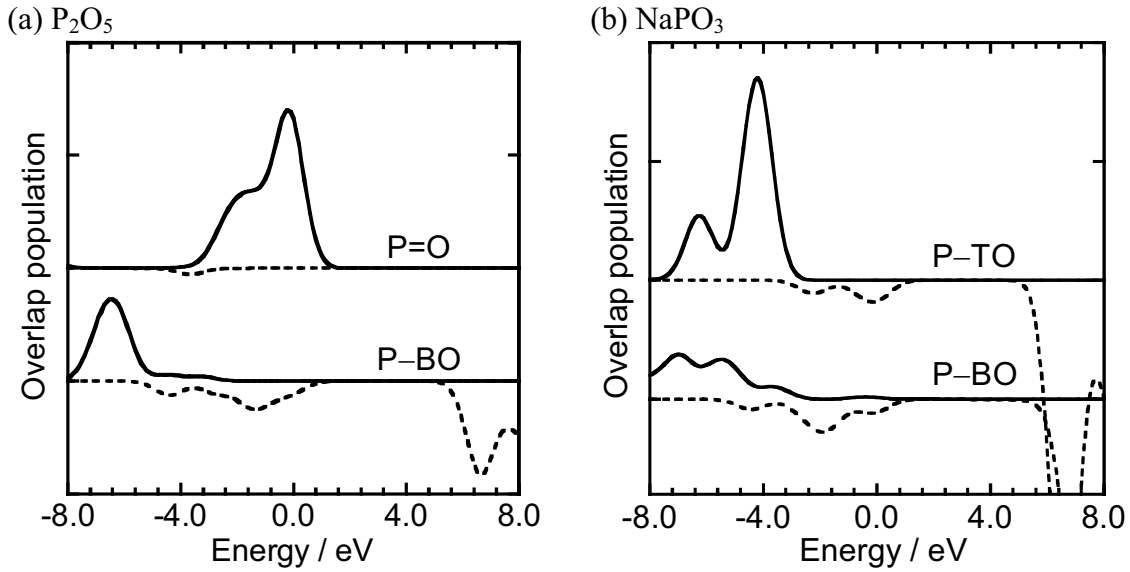

Figure 3: Overlap population diagrams for P–O bonds in some phosphate crystals.
(a) P_2O_5, (b) $NaPO_3$ and (c) $Na_5P_3O_{10}$.
The continuous and broken lines indicate bonding and anti-binding overlap, respectively.

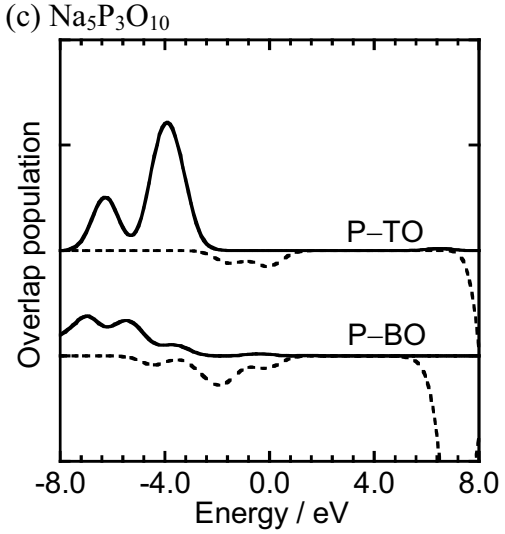

Figure 3: (continuation)

Chemical Bonding Character of Aluminophosphates

The results of aluminophosphates are shown in Figure 4. It should be noted that the Q_{MO} values shown in Fig. 4 are obtained only from P–O and Al–O bonds in P–O–Al bridges, and Q_{PO} of P–O bonds in P–O–P bridges are not indicated in Fig. 4. With increasing Al/P atomic ratio, Q_{MO} of Al–O bonds increases and that of P–O bonds decreases. In general, tetrahedral and octahedral Al atoms have been regarded as network formers and modifiers, respectively, and hence oxygen atoms in P–O–Al(4) and P–O–Al(6) bridges are regarded as BOs and NBOs, respectively. Therefore, the result observed in Fig. 4, that is, Q_{PO} for P–O–Al(4) bridges in $AlPO_4$ is smaller than that for P–O–Al(6) bridges in $NaAlP_2O_7$ and $Al(PO_3)_3$, seems plausible.

In an aluminosilicate $KNa_3Al_4Si_4O_{16}$ [18], Q_{SiO} and Q_{AlO} for Si–O–Al(4) bridges are 0.62 and 0.39, respectively. Comparing the P–O–Al(4) and Si–O–Al(4) bridges, Q_{AlO} are almost the same value, but Q_{PO} is much larger than Q_{SiO}. In PO_4 units in $AlPO_4$, all oxygen atoms are in P–O–Al(4) bridges, and no terminal oxygen atoms are present. If π-bonding electrons originally localized on a P=O bond in a PO_4 unit are evenly delocalized among the four P–O bonds, the bond order of P–O bonds will be 1.25. The larger bond order of P–O bonds leads to the larger Q_{PO} in $AlPO_4$.

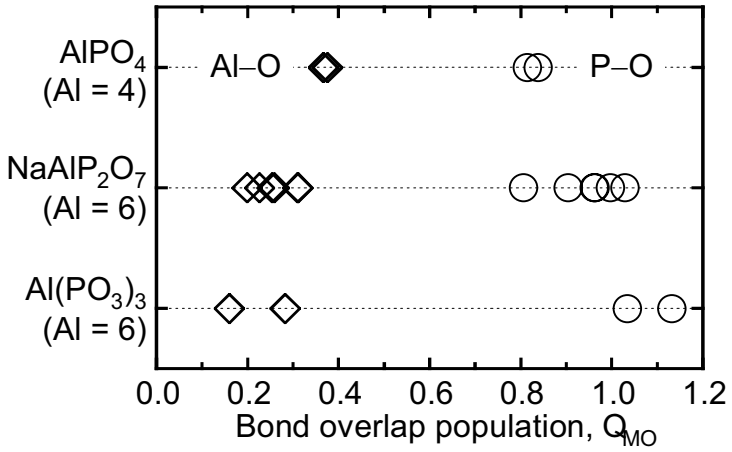

Figure 4: Bond overlap population, Q_{MO} of P–O and Al–O bonds in P–O–Al bridges in the aluminophosphate crystals.

Chemical Bonding Character of Phosphates Containing Other Network Formers

It is well known that even the conventional network formers of B, Si and Ge atoms occupy higher coordination sites when small amount of the respective oxides are added to a phosphate glass. To the best of the authors' knowledge, B, Si and Ge atoms have higher coordination numbers in crystalline phosphates. Then, chemical bonding character of P–O–M bridges (M = B(4), Si(6) and Ge(6)) was investigated. As shown in Figure 5, Q_{PO} is larger than Q_{MO} in every P–O–M bridge, which is probably due to the larger electronegativity of P (2.19) compared with the other network forming atoms (B = 2.04, Al = 1.61, Si = 1.90, Ge = 2.01), where Pauling electronegativities [20] are indicated. Electrons on P–O–M bridges gravitate toward more electronegative P atoms, resulting in larger Q_{PO} than Q_{MO}. Thus, less electrons are localized on M–O bonds in P–O–M bridges, and hence more M–O bonds are required to compensate the positive charge of central M atoms, resulting in the higher coordination numbers of M. As also shown in Fig. 5, Q_{PO} and Q_{MO} are ranked in ascending and descending orders of P–O–B(4), P–O–Si(6) and P–O–Ge(6), respectively, and the difference between Q_{PO} and Q_{MO} increases in that order. If the electronegativity of Ge were between Al and Si, the difference in bond overlap population would be in consistent with the difference in electronegativity. [20].

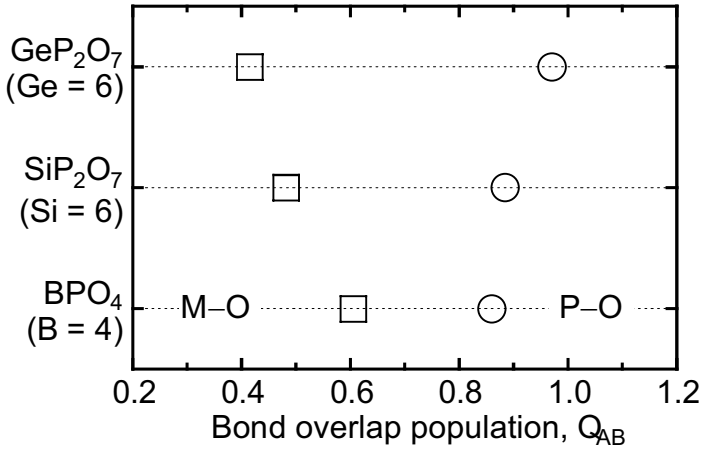

Figure 5: Bond overlap population, Q_{AB} of P–O and M–O bonds in P–O–M bridges in the phosphate crystals.

Conclusion

Molecular orbital calculations have been performed to investigate the chemical bonding character of phosphate glasses, where cluster models were constructed based on the phosphate crystals. The chemical bonding character was evaluated by the bond overlap population Q_{AB}. Q_{PO} of P=O double bonds was much larger than those of terminal B–NBO and Si–NBO bonds, which was due to the larger bond order of P=O double bonds. By addition of alkali oxides, Q_{PO} of the terminal P–TO (P=O + P–NBO) bonds decreased, which was characteristic in phosphate system because in silicate system Si–NBO bonds increased in Q_{SiO} with increasing alkali content. According to overlap population diagram, anti-bonding overlap of Si and O orbitals in Si–NBO bonds was not observed at around HOMO levels, and in P–TO bonds, however, anti-bonding overlap was clearly seen, which probably lead to the unique change in Q_{PO} in the phosphate system. P–O–P bridging bonds in pure P_2O_5 crystal indicated much highest Q_{AB} as compared with the bridging bonds in B_2O_3, SiO_2 and GeO_2 crystals, suggesting the highest bond covalency among the conventional glass formers.

As for P–O–Al bridges in aluminophosphates, Q_{PO} in P–O–Al(4) was smaller than that in P–O–Al(6),

suggesting the delocalization of electrons through tetrahedral Al atoms. Q_{PO} was higher than Q_{AlO} regardless of the coordination number of Al atoms. Such the disproportionate sharing of electrons in P–O–M bridges was also found in the cases of M = B(4), Si(6) and Ge(6) as well as Al(4) and Al(6). In every combination, Q_{PO} was always larger than Q_{MO}, which was responsible for larger electronegativity of P atom. Less Q_{MO} in P–O–M bridges was also responsible for the preferential occupation in higher coordination sites of M atoms in phosphate glasses.

References

1. T. Nanba, Y. Miura, S. Sakida, "Consideration on the correlation between basicity of oxide glasses and O1s chemical shift in XPS," J. Ceram. Soc. Japan, 113(1) (2005) 44-50.
2. T. Tanaka, "Electronic structure of alkali phosphate glasses," (M.S. thesis, Okayama University, 1998).
3. T. Uchino, Y. Ogata, "Ab initio molecular orbital calculations on the electronic structure of phosphate glasses. Binary alkali metaphosphate glasses," J. Non-Cryst Solids, 191 (1995) 56-70.
4. H. Adachi, M. Tsukada, C. Satoko, "Discrete Variational Xα Cluster Calculations. I. Application to Metal Clusters," J. Phys. Soc. Japan, 45 (1978) 875-883.
5. R.S. Mulliken, "Electronic Population Analysis on LCAO-MO Molecular Wave Functions," J. Chem. Phys., 23, (1955) 1833-1840, 1841-1846, 2338-2342, and 2343-2346.
6. D. Stachel, I. Svoboda, H. Fuess, "P_2O_5-3 V, e12." Acta Cryst., C51 (1995) 1049.
7. O.G. Bondareva, M.A. Simonov, H.B. Belov, Dokl. Akad. Nauk. SSSR, 240 (1978) 75-77.
8. K.H. Jost, "Die Struktur des Kurrol'schen Na-Salzen $(NaPO_3)_x$ Typ A," Acta Cryst., 14 (1961) 844-847.
9. D.R. Davies, D.E.C. Corbridge, "The Crystal Structure of Sodium Triphosphate, $Na_5P_3O_{10}$, Phase II," Acta Cryst., 11 (1958) 315-319.
10. K.H. Jost, "Die Struktur des Kaliumpolyphosphats $(KPO_3)_x$," Acta Cryst., 16 (1963) 623-626.
11. D.E.C. Corbridge, "The Crystal Structure of Rubidium Metaphosphate," Acta Cryst., 9 (1956) 308-314.
12. L. Pauling, J. Sherman, "The Crystal Structure of $Al(PO_3)_3$" Z. Krist., 96A (1937), 481
13. J. Alkemper, H. Paulus, H. Fuess, "Crystal structure of aluminium sodium pyrophosphate, $NaAlP_2O_7$." Z. Krist. 209 (1994), 616-616.
14. M. Strada, "The Crystal Structure of Some Phosphates and Arsenates of Trivalent Metals. I. Phosphate and Arsenate of Aluminum($AlPO_4$ and $AlAsO_4$)," Gazz. Chim. Ital., 64(1934), 653
15. F. Dachille, L.S.D. Glasser, "High pressure forms of BPO_4 and $BAsO_4$; quartz analogues," Acta Cryst., 12 (1959) 820-821.
16. G. Bissert, F. Liebau, "Die Kristallstruktur von monoklinem Siliziumphosphate SiP_2O_7 AIII: Eine Phase mit $[SiO_6]$-Oktaedern," Acta Cryst. B26, (1970) 233-240.
17. A. Burdese, M.L. Borlera,"Crystallographic Characteristics of the Cubic and Orthorhombic Forms of Thorium Pyrophosphate,"Atti Accad. Sci. Torino, Classe Sci. Fis. Mat. Nat., 94 (1960), 89.
18. T. Nanba, S. Sakida, Y. Miura, "Chemical bonding character of the network forming bonds in oxide glasses," Proceedings in Pacrim6, Maui, Hawaii, (2005) S5-17-I

19. T. Nanba, T. Hagiwara, Y. Miura, “Chemical bonding state of sodium silicates,” Advances in Quantum Chemistry, 42 (2003) 187-198.
20. A.L. Allred, “Electronegativity values from thermochemical data,” J. Inorg. Nucl. Chem., 17 (1961) 215-221.